Steel and Composite Structures, Vol. 13, No. 6 (2012) 587-606
DOI: http://dx.doi.org/10.12989/scs.2012.13.6.587

Uni-axial behaviour of normal-strength CFDST columns with external steel rings

C.X. Dong and J.C.M. Ho*

Department of Civil Engineering, The University of Hong Kong, Hong Kong

(Received April 02, 2012, Revised October 27, 2012, Accepted November 05, 2012)

Abstract. Concrete-filled-steel-tubular (CFST) columns have been well proven to improve effectively the strength, stiffness and ductility of concrete members. However, the central part of concrete in CFST columns is not fully utilised under uni-axial compression, bending and torsion. It has small contribution to both flexural and torsion strength, while it can be replaced effectively by steel with smaller area to give similar load-carrying capacity. Also, the confining pressure in CFST columns builds up slowly because the initial elastic dilation of concrete is small before micro-crackings of concrete are developed. From these observations, it is convinced that the central concrete can be effectively replaced by another hollow steel tube with smaller area to form double-skinned concrete-filled-steel-tubular (CFDST) columns. In this study, a series of uni-axial compression tests were carried out on CFDST and CFST columns with and without external steel rings. From the test results, it was observed that on average that the stiffness and elastic strength of CFDST columns are about 25.8% and 33.4% respectively larger than CFST columns with similar equivalent area. The averaged axial load-carrying capacity of CFDST columns is 7.8% higher than CFST columns. Lastly, a theoretical model that takes into account the confining effects of steel tube and external rings for predicting the uni-axial load-carrying capacity of CFDST columns is developed.

Keywords: columns; concrete-filled; double-skin; normal-strength concrete; rings.

1. Introduction

It has been commonly accepted that the strength, stiffness and ductility of reinforced concrete members can be significantly improved by installing transverse confinement to confine the concrete core (Lee 2007, Lu and Zhou 2007, Bindhu *et al*. 2008, Bechtoula *et al*. 2009, Zhang *et al*. 2009, Sadjadi and Kianoush 2010, Ho 2011) within prescribed critical region length (Pam and Ho 2009, Yan and Au 2010, Zhao *et al*. 2012). Traditionally, the confinement was provided by installing transverse steel (or stirrups) at close spacing to confine the core concrete (Pam and Ho 2001, Ho *et al*. 2010, 2012, Lam *et al*. 2009, 2009b, Zhou *et al*. 2010). However, the major disadvantage of this form of confinement is that the core concrete in both the horizontal and vertical planes between the laterally restrained transverse steel is not effectively confined owing to arching action (Mander *et al*. 1988). Therefore, the effectively confined concrete is smaller than the core concrete area, and the effectiveness reduces significantly as the spacing of transverse steel increases. To improve the efficiency of concrete core confinement, concrete-filled-steel-tubular (CFST) column that consists of a hollow steel tube with

* Corresponding author, Assistant Professor, E-mail: johnny.ho@hku.hk

concrete filled inside was advocated (Huang *et al*. 2008, Yang and Han 2008, Fang and Zhu 2009, Han *et al.* 2009, Dai and Lam 2010, Hu *et al*. 2010, Park *et al*. 2010). The major advantages of CFST columns are that: (1) It provides a more uniform and continuous confining pressure to the concrete inside such that the confinement effectiveness increases (i.e., minimising arching action). (2) The steel tube acts as both the longitudinal and confining reinforcement that enhances the strength-to-weight ratio of the column. (3) The steel tube acts as formwork such that no external formwork for concreting is required. It saves the construction materials and shortens the construction cycle time. (4) The floor area saved due to the enhanced strength is always beneficial to the developers, architects and engineers.

However, CFST columns have some disadvantages: (1) Under uni-axial compression, steel sustains more load than concrete does (per same area) because of higher stiffness under composite action. (2) Under flexure, the central concrete that is close to the neutral axis contributes less to the flexural strength than that close to the extreme fibre because of shorter lever arm. (3) Under torsion, the central concrete has small contribution to the torsion strength. (4) The initial elastic dilation of concrete is quite small and thus the building up of confining pressure provided by the steel tube is slow. It only develops more rapidly until micro-crackings of concrete have been formed (Wei *et al.* 1995a, 1995b) at large strain. (5) The self weight of CFST columns is quite heavy, which is mainly due to the self-weight of the in-filled core concrete. From the above observations, it is evident that the central concrete can be effectively replaced by another hollow steel tube with smaller area, while maintaining similar uni-axial, flexure and torsion strength. By replacing part of the central concrete core with an inner hollow steel tube, this form of column construction is known as double-skinned concrete-filled-steel-tubular (CFDST) columns.

CFDST column is a composite member, which consists of inner and outer steel skins with the annulus between the skins filled with concrete. From structural point of view, this form of column has higher strength (uni-axial, flexural and torsion) (Young and Ellobody 2006, Choi *et al*. 2007), ductility and energy absorption before failure (Elchalakani *et al.* 2002, Zhao and Grzebieta 2002, Hsu *et al*. 2009, Uenaka *et al.* 2010, Zhao *et al.* 2010). By replacing the central concrete with a steel tube of much smaller cross-section area, the strength-to-weight ratio of the columns is improved significantly. Furthermore, the inner tube expands laterally during compression and hence increases the confining pressure provided to the concrete. Thus, the initial confining pressure builds up more rapidly than that in CFST columns. From environmental point of view, CFDST column consumes less concrete (replaced by steel with about 1/6 section area), which reduces the embodied carbon and energy levels of the columns. It also generates less demolition waste as steel is more recyclable than concrete. Lastly, the cavity in the inner tube provides a dry atmosphere for possible catering of facilities or utilities like power cables, telecommunication lines and drainage pipes. This form of construction is particularly useful for maritime structures in which the sub-sea facilities can be accommodated in the dry atmosphere provided by the inner cavity. An alternative form of double-skin structures is the sandwich structures, in which concrete is filled within two steel plates – “panels” (Liew and Sohel 2009, 2010, Liew *et al*. 2009, Sohel and Liew 2011). However in this type of structure, the confinement provided to the concrete is not significantly improved because the panels are not closed sections. This form of construction is more popular in horizontal flexural member but less in vertical flexural members such as columns owing to the presence of compressive axial load.

There were already some tests conducted on unconfined CFDST columns in the past (Wei *et al.* 1995, Elchalakani *et al.* 2002, Han *et al.* 2004, Tao *et al.* 2004, Uenaka *et al*. 2008) in terms of the uni-axial strength and stiffness. However, the confinement was not fully utilised in these columns because the steel-concrete interface bonding during initial elastic stage was not intact due to the difference in

Poisson's ratios of the materials (Persson 1999, Ferretti 2004, Lu and Hsu 2007). The elastic strength and stiffness were therefore considered not fully developed. To resolve this problem, the authors recommend adding external steel rings to confine CFDST columns so as to maintain an intact interface bonding during initial elastic compression by providing extra confining pressure. Previously, some similar efforts have been carried out to improve the interface bonding. For example, Cai and He (2006) investigated the axial load behaviour of square concrete-filled tubular stub column with binding bars as confinement. It was reported that the CFT stub column without binding bars failed with a lower strength and ductility, while the improvement in ultimate strength of columns with binding bars could reach 40%. However, for this type of columns, holes were drilled on the external steel tube that reduced the load-carrying capacity of the column. Similar results were also obtained by Tao *et al.* (2007). As an alternative to steel binding bars, external steel rings are adopted herein to confine the outer steel tube and in-filled concrete, which provide a more uniform and continuous confining pressure than the binding bars. More importantly, there is no need to drill holes on the outer steel tube and hence the column will not be weakened.

In this study, the uni-axial behaviour of ring-confined CFDST columns will be investigated in terms of load-carrying capacity, elastic strength (measured at 0.2% proof strain) and stiffness. From the experimental results, it was observed that the elastic strength and stiffness of the CFDST columns were on average 33.4% and 25.8% respectively larger than those of the counterpart CFST columns with the same equivalent section area. Also, it was seen that the confining stress in the outer tube of the CFDST columns builds up more rapidly than the counterpart CFST columns under similar axial strain. Lastly, a theoretical model for evaluating the load-carrying capacity of unconfined and confined CFDST columns is proposed for design purpose. The validity of the theoretical model is verified by comparing the predicted strength with the authors' obtained test results and those from other researchers on CFDST columns with or without external steel rings.

2. Experimental programme

2.1 Details of the specimens

In this paper, a total of ten normal-strength CFST and CFDST column specimens have been fabricated and tested. The specimens can be divided into three groups: (1) four normal-strength CFST columns with different spacing ($5t$, $10t$, $15t$ and $20t$, t is the thickness of the steel tube) of external steel rings; (2) four normal-strength CFDST columns with different spacing ($5t$, $10t$, $15t$ and $20t$) of external steel rings; (3) one normal-strength CFST column and one normal-strength CFDST column without external steel rings. The concrete cube and cylinder strength were about 60 MPa and 50 MPa on the testing day. The grade of steel is S355 produced as per BS EN 10210-2:2006. For CFST columns, the thickness of the steel tubes is 10 mm and the outer diameter is 139.7 mm. For CFDST columns, the thickness of the inner and outer tubes is 5 mm. The outer diameters of the inner and outer tubes are 88.9 mm and 168.3 mm respectively. Fig. 1(a) shows the CFST column specimens with external steel rings. Fig. 1(b) shows the CFDST column specimens with external steel rings. Figs. 1(c) and 1(d) show respectively the CFDST and CFST column specimen without external steel rings. Fig. 1(e) shows the photo of the hollow steel tubes. The sectional and material properties of the specimens are summarised in Table 1.

The external steel rings were made of mild steel round bars of 8 mm diameter. The yield strength of

Fig. 1(a) CFST columns with external steel rings (s=5t, 10t, 15t and 20t)

Fig. 1(b) CFDST columns with external steel rings (s= 5t, 10t, 15t and 20t)

Fig. 1(c) CFST columns without external steel ring

Fig. 1(d) CFDST columns without external steel ring

Fig. 1(e) Hollow steel tubes (Diameter = 168.3 mm, 88.9 mm and 139.7 mm)

the steel bars is f_R = 300 MPa. The rings were welded to the outer tubes at different spacing. Each ring was welded to the outer steel tube at 8 locations in one level, which were separated from each other at 45^o from the centre of specimen.

A naming system consisting of a letter and three numbers is used to represent the specimens. For instance, 'D-50-5-5' represents a CFDST column (indicated by the first letter "D"), a concrete cylinder strength of about 50 MPa at the testing day (indicated by the first number "50"), thickness of both inner

Table 1 Details of specimens and materials summary

Specimen label	D_i (mm)	t_i (mm)	$f_{y,i}$ (MPa)	D_o (mm)	t_o (mm)	$f_{y,o}$ (MPa)	f_c (MPa)	f_R (MPa)
D-50-5-5	88.9	5	450	168.3	5	360	50	300
D-50-5-10	88.9	5	450	168.3	5	360	50	300
D-50-5-15	88.9	5	450	168.3	5	360	50	300
D-50-5-20	88.9	5	450	168.3	5	360	50	300
D-50-5-0	88.9	5	450	168.3	5	360	50	-
C-50-10-5	-	-	-	139.7	10	360	50	300
C-50-10-10	-	-	-	139.7	10	360	50	300
C-50-10-15	-	-	-	139.7	10	360	50	300
C-50-10-20	-	-	-	139.7	10	360	50	300
C-50-10-0	-	-	-	139.7	10	360	50	-

and outer tubes of 5 mm (indicated by the second number “5”), and lastly five times the thickness of steel tube for the ring spacing (indicated by the last number“5”). Alternatively, ‘C-50-10-0’ represents a CFST column (indicated by the first letter “C”) with concrete cylinder strength of about 50 MPa (indicated by the first number “50”), a thickness of the steel tube of 10 mm (indicated by the second number “10”), and lastly no external steel ring was provided (i.e., zero spacing indicated by the last number “0”).

Three plain concrete cylinders (150 × 300 mm) were tested in a 5,000 kN compression machine on the testing day to obtain the uni-axial compressive strength as well as the elastic modulus of concrete. Apart from concrete cylinders, three 150 mm concrete cubes were also tested to obtain the concrete cube strength on the testing day for reference purpose.

2.2 Instrumentation

The following instrumentation was adopted in this study:

a) Strain gauges – Two-dimensional strain gauges of type FCA-5-11-3L produced by Tokyo Sokki Kenkyujo Co., Ltd were adopted to measure the strain of the longitudinal and transverse strains of the specimens. Three strain gauges were installed at the mid-level of the outer tube with 120º separated from each other from the centre of the specimen. Fig. 2 shows the details of the strain gauges.

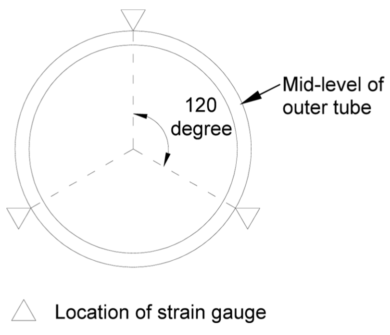

Fig. 2 Details of installation of strain gauges

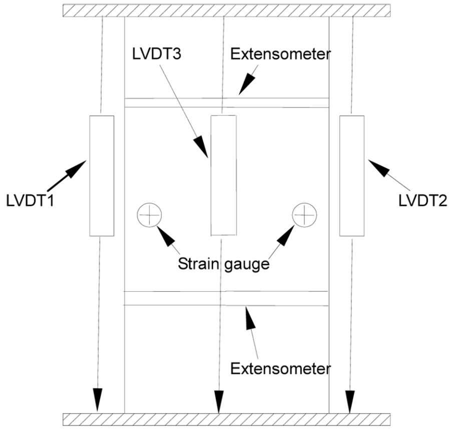

Fig. 3 Details of installation of LVDTs and circumferential extensometers

b) Linear variable differential transducers (LVDTs) – Three LVDTs with 100 mm stroke were used to measure the axial shortening of the specimen during the test. They were installed to measure the movement of the bottom plate relative to the top plate, which were separated from each other with an angle of 120^{o} at the centre of the specimen. The average value of the readings obtained from these LVDTs would be taken as the measured axial shortening of the specimen. Fig. 3 shows the details of the LVDTs.

c) Circumferential Extensometer – Circumferential extensometers were used to measure the lateral expansion of the specimens within the elastic stage. The circumferential extensometers were removed when the measured lateral expansion was about to reach 6 mm, which is the maximum limit of the range of measurement. For unconfined and ring-confined CFDST and CFST specimens, two circumferential extensometers were installed at the locations which are 1/3 and 2/3 of the total height of the specimens to avoid clashing with the external steel rings. The installation details of the circumferential extensometers are also shown in Fig. 3.

Fig. 4 Photo of compression machine

2.3 Testing procedure

The compression test was carried out by a 5,000 kN compression machine (see Fig. 4). The test was conducted under displacement control. The initial loading rate was 0.3 mm/min and increased incrementally by 0.05 mm/min for every 10 mm axial deformation after the specimen had yielded. The loading application would be stopped when the applied load dropped to 80% of the maximum measured load of the specimens or when the displacement reached about 60 mm, whichever was earlier. For concrete cylinders, the loading rate was set constant at 0.3 mm/min.

3. Experimental results

3.1 Lateral elastic dilation of CFDST and CFST

The lateral deformations of the unconfined CFDST and CFST specimens (i.e., D-50-5-0 and C-50-10-0) are plotted in Figs. 5(a) and 5(b) at different measured axial shortening from 0.3 mm to 1.5 mm. The measured axial shortening was taken as the average value of the readings obtained by the three LVDTs. In these figures, the *y*-axis represents the distance from the base of the specimens, while the *x*-axis represents the measured lateral strain. The lateral strain was taken as average of the strain measured by the circumferential expansion divided by the circumferential length as well as the strain gauges at mid height of the specimens. From Figs. 5(a) and 5(b), it can be found that at the axial shortening of 0.5 mm, the maximum lateral strains are 456 με and 380 με for D-50-5-0 and C-50-10-0 respectively. When the axial shortening increased to 1.5 mm, the maximum lateral strains increased to 1597 με and 913 με for D-50-5-0 and C-50-10-0 respectively that indicated the lateral dilation of CFDST specimen was about 75% larger than the CFST specimen with the same equivalent area. Hence, the lateral dilation in CFDST column built up more rapidly than that in the CFST column under compression. Consequently, the concrete in CFDST columns would be subjected to a larger confining pressure produced by the outer tube in CFDST column. This phenomenon was believed to be caused by the lateral expansion of the inner tube under compression, which pushed the in-filled concrete towards the outer tube. It thus verifies that CFDST column is able to provide a better confinement to the

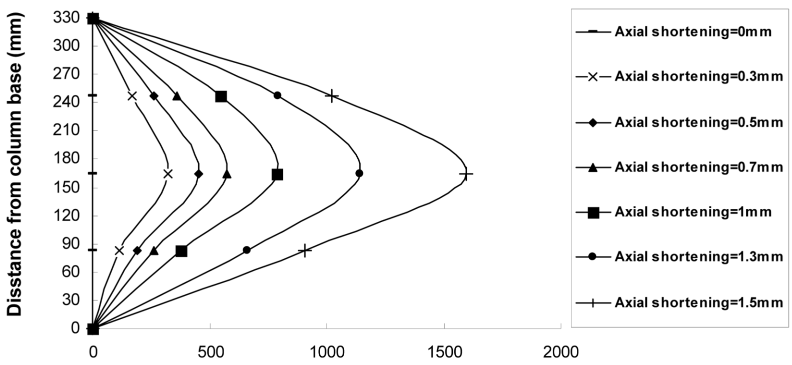

Fig. 5(a) Transverse strain at different axial shortening of D-50-5-0

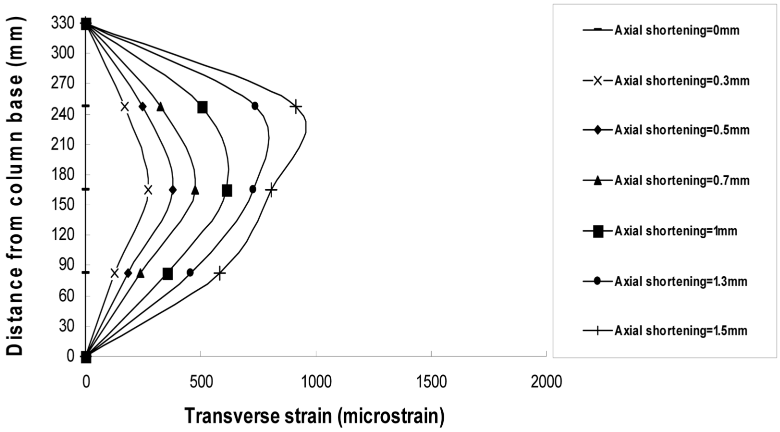

Fig. 5(b) Transverse strain at different axial shortening of C-50-10-0

concrete core than CFST column.

3.2 Axial load against axial shortening curves of CFDST and CFST

Fig. 6(a) shows the graphs plotting the measured axial load against the axial shortening for the unconfined CFDST column and ring-confined CFDST columns with various ring spacing (i.e., $5t$, $10t$, $15t$ & $20t$). The y-axis represents the axial load measured during the test while the x-axis represents the axial shortening measured by the LVDTs, the latter of which was taken as the average of the LVDT readings. From the figure, it can be seen that the ring-confined CFDST columns had larger elastic strength (defined as 0.2% proof stress), elastic stiffness and ductility than the unconfined CFDST column (except for the D-50-5-20 which had a smaller elastic strength because of poor compaction during concreting that affected the strength of concrete).

It is also observed from Fig. 6(a) that the axial load-carrying capacity and ductility of CFDST

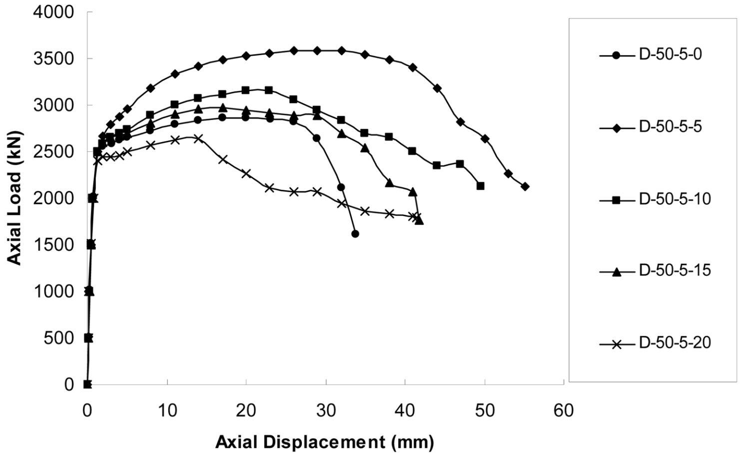

Fig. 6(a) Load displacement curves of CFDST columns

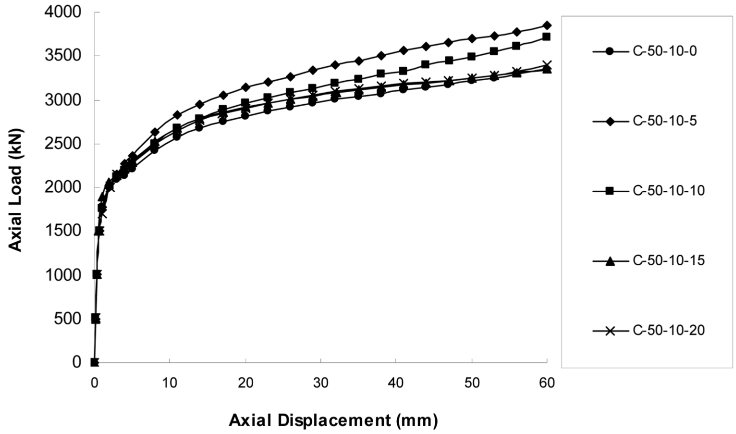

Fig. 6(b) Load displacement curves of CFST columns

columns increases as the spacing of ring confinement reduces. The axial load-carrying capacity, which is defined as the measured strength at 0.05 axial strain (0.05 axial strain is adopted as one-half of the fracture strain of steel and is normally adequate for design of flexural members), was 3464 kN for D-50-5-5. This is because when the spacing of rings reduced, the steel tube and the concrete core were subjected to a larger, more uniform and continuous confining pressure that enhanced the compressive axial strength of steel tube and concrete. The reduced spacing also decreases the effective length of columns to the same as the ring spacing, which significantly increases the buckling load of the steel tube to avoid instability. The increase in confining pressure would also restrict the lateral dilation of the CFDST columns and hence the axial shortening at a given applied axial load. This implies that the elastic stiffness of the ring-confined CFDST column was also improved.

Fig. 6(b) shows the load-displacement curves of the CFST columns, which were designed and fabricated such that they have the same equivalent cross-section area as the respective CFDST columns with the same ring spacing in terms of tube thickness. Similarly, the axial load-carrying capacity of CFST columns, which is defined similarly as the measured strength at 0.05 axial strain, increases as the spacing of ring confinement reduces due to the same reason as for the CFDST columns. The largest axial load-carrying capacity obtained was 3031 kN for C-50-10-5.

Comparing Figs. 6(a) with 6(b), it is evident that the axial strength develops more rapidly in the CFDST column at initial stage than that in the respectively CFST column with the same equivalent area and ring-spacing-to-thickness ratio (i.e., higher strength was developed for a given axial displacement during initial stage). It may be due to the fact that for CFDST columns, the inner tube also expanded under compressive axial load and thereby pushing outward against the concrete, which were in turn confined by the outer steel tube. Provided that the outer steel tube did not buckle, the expansion of the inner tube would increase the confined concrete stress and hence the load-carrying capacity. More importantly, the prevention of outward buckling of the inner tube provided by the concrete would increase the axial strength of the inner tube, which in turn increased the axial load-carrying capacity of the CFDST column. Despite the improvement in axial strength, it was however observed that the strength degradation of CFDST columns occurred earlier than that in the CFST columns. The reason was because of the very high axial stress carried by the inner tube of the CFDST column when compared with that carried by the equivalent concrete area in the respective CFST column. Once the inner tube failed at large applied load, the load taken up by the outer tube and concrete would be increased abruptly that caused the failure of the outer tube and hence the column. Nonetheless, it was observed that the strength degradation only occurred at an axial displacement of about 30 mm (or axial strain = 0.09), which is considered very high and normally will not be reached in the flexural members.

3.3 Elastic strength, load-carrying capacity and stiffness enhancement

As mentioned previously, it is clear that CFDST columns develop strength more rapidly than CFST columns at early elastic stage. This has been indirectly verified by the larger measured lateral dilation in CFDST columns than that in the respective CFST columns (see Fig. 5) such that the confining pressure and thus the axial strength of CFDST columns were larger. For direct verification, the elastic strength at 0.2% strain is determined in this section for each of the test specimens to illustrate the extent of strength development at early elastic stage. Table 2 summarises the obtained values of the elastic strength. From the table, it is evident that the elastic strength obtained for the CFDST columns is larger than those of the respective CFST columns with the same equivalent section area. The average difference between the obtained elastic strength of CFDST and CFST columns is about 33.4%. The maximum difference obtained is about 41.7%.

Table 2 also shows the load-carrying capacity (taken as the measured load at 0.05 axial strain) of the CFDST columns. From the table, it is seen that the axial load-carrying capacity obtained for the CFDST columns are larger than those of the respective CFST columns with the same equivalent section area. The average difference between the obtained load-carrying capacity of CFDST and CFST columns is about 7.8%, while the maximum difference is 14.3% for D-50-5-5 and C-50-10-5.

Table 3 summarises the elastic stiffness obtained for the tested CFDST and CFST columns. The elastic stiffness of the specimens was obtained by the slope of the initial straight line portion in the load-displacement curve. From the table, it is obvious that the elastic modulus obtained for the CFDST columns are larger than those of the respective CFST columns counterparts. The average difference between the obtained elastic modulus of CFDST and CFST columns is about 25.8%, while the maximum difference is 45.6% for D-50-5-5 and C-50-10-5.

Table 2 Elastic strength and load-carrying capacity enhancement ratios

Specimen label	Elastic strength (kN)	Enhancement ratio (%)	Load-carrying capacity (kN)	Enhancement ratio (%)
D-50-5-5	2444	30.0	3464	14.3
C-50-10-5	1880		3031	
D-50-5-10	2500	33.8	3107	8.4
C-50-10-10	1869		2865	
D-50-5-15	2515	28.0	2971	4.6
C-50-10-15	1965		2841	
D-50-5-20	---*	---*	---*	---*
C-50-10-20	1826		2825	
D-50-5-0	2520	41.7	2852	4.0
C-50-10-0	1779		2742	
Average		33.4		7.8

*Result is NOT included because of poor concrete compaction.

Table 3 Elastic stiffness enhancement ratios

Specimen label	Stiffness (kN/mm)	Stiffness enhancement ratio (%)
D-50-5-5	4437	45.6
C-50-10-5	3047	
D-50-5-10	4072	29.8
C-50-10-10	3136	
D-50-5-15	3979	16.5
C-50-10-15	3416	
D-50-5-20	---*	---*
C-50-10-20	3120	
D-50-5-0	3339	11.4
C-50-10-0	2998	
Average		25.8

*Result is NOT included because of poor concrete compaction.

3.4 Failure mode

Fig. 7(a) shows the failure modes of the unconfined CFDST and CFST columns. From the figure, it is observed that the failure mode of unconfined CFST column was the overall buckling of the outer steel tube without fracture, whereas as that of the unconfined CFDST column was the fracture of the outer steel tube. For the CFST column, the outer steel tube buckled under large axial strain when the concrete crushed within the steel tube. Since the tube was unconfined, the effective length was equal to the overall height of the column, and overall buckling occurred. (Note: Elephant-foot buckling was observed at both ends of the columns which was the elastic-plastic collapse of axially-loaded steel tube subjected to internally pressure due to expansion/crushing of concrete adjacent to the end supports). For the CFDST columns, it can be seen from Fig. 7(a) that the outer steel tube fractured during the failure of the column. This was because the thickness of the inner tube was designed such that it would fail before the outer tube. Once the inner tube failed, a large amount of axial load was immediately transferred to

Fig. 7(a) Failure modes of unconfined CFST and CFDST column

Fig. 7(b) Failure modes of CFDST columns with external steel rings

Fig. 7(c) Failure modes of CFST columns without external steel rings

the concrete and outer tube. Then, the outer tube was subjected to an abrupt increase in the axial stress as well as hoop splitting tensile stress, which eventually caused fracture of the outer steel tube in the longitudinal direction.

Figs. 7(b) and 7(c) shows the failure mode of ring-confined CFDST and CFST columns respectively. The failure modes of ring-confined CDFST and CFST columns, in which only local buckling between the rings was observed, are different from those of unconfined counterparts. This was because the external rings provided effective lateral restraints against buckling for the steel tube. It limited the effective length to the ring spacing and hence increased the column buckling load. Fracturing of outer steel tube was also observed for the ring-confined CFDST columns due to the larger additional axial load and hoop tensile splitting stress transferred by the inner tube when it failed. However, the same failure mode was not observed for CFST columns with rings because there was no abrupt increase in the steel stress during failure.

4. Proposed analytical model for uni-axial strength prediction of CFDST columns

4.1 Proposed analytical model

In this study, the uni-axial behaviour of unconfined and ring-confined CFDST columns has been investigated experimentally. Previously, no analytical model has been presented to predict the uni-axial strength of CFDST columns installed with external steel rings. Therefore in this study, a numerical model is proposed that is applicable to predict the uni-axial strength of both unconfined and confined CFDST columns. The model takes into account the enhancement of the axial strength of both the inner and outer steel tubes as well as the core concrete by considering the confining pressure provided by the external rings. The overall axial load-carrying capacity of the CFDST columns is taken as the summation of the enhanced axial strength of both the outer and inner steel tubes as well as confined concrete core.

The overall formula for evaluating the axial capacity of the CFDST columns is shown in Eq. (1), which is the approach commonly adopted by previous researchers (Wei *et al.* 1995a, 1995b, Tao *et al.* 2004).

$$N = N_i + N_o + N_{cc} \tag{1}$$

$$N_i = f_i A_i \tag{2a}$$

$$N_o = f_o A_o \tag{2b}$$

$$N_{cc} = f_{cc} A_{cc} \tag{2c}$$

where N, N_i, N_o and N_{cc} in Eq. (1) represent the axial load sustained by the CFDST column, inner steel tube, outer steel tube and core concrete respectively. In Eq. (2), f_i and f_o are the axial stresses in the inner and outer tubes respectively under bi-axial stress state; f_{cc} is the axial stress in the core concrete under the confining stress f_r. A_i, A_o and A_{cc} are the cross-section areas of the inner tube, outer tube and the core concrete respectively. In this model, it is assumed that due to the uniform and continuous confining pressure provided by the steel tubes, the variation of confining pressure along the column height is so small that it can be regarded as relatively constant along the column height. It should also be noted that both inner and outer tubes were subjected to bi-axial stress. The inner tube was subjected to hoop compressive stress due to the confinement provided by the core concrete and axial compressive stress due to axial load, whereas the outer tube were subjected to hoop tensile stress and axial compressive stress. Fig. 8(a) shows the free body diagram of the inner tube subjected to confining pressure f_r. The hoop compressive stress developed in the inner tube is denoted by $\sigma_{\theta ji}$. By considering the force equilibrium of the inner tube, Eq. (3) can be established.

$$\sigma_{\theta,i} = \frac{f_r D_i}{2t_i} \tag{3}$$

where D_i is the diameter of the inner tube and t_i is the thickness of the inner tube. On the other hand, the hoop tensile stress developed in the outer tube can be derived by considering the force equilibrium of the outer tube under the confining pressure provided by the concrete, the hoop tensile stress provided by the outer tube and the external rings. The free body diagram of the outer tube with rings is shown in Fig. 8(b). Eqs. (4a) and (4b) show the force equilibrium equations

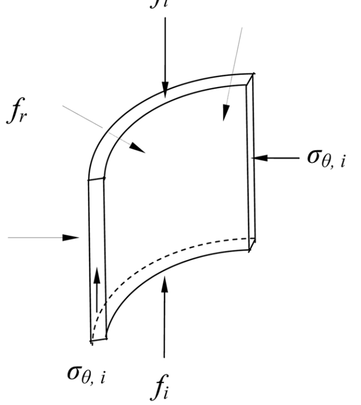

Fig. 8(a) Free body diagram of the inner tube

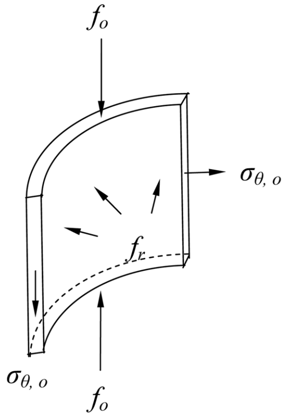

Fig. 8(b) Free body diagram of the outer tube

$$-(2\sigma_{\theta,o}t_o h + 2nA_R\sigma_R) = f_r(D_o - 2t_o)h \tag{4a}$$

$$\sigma_{\theta,o} = -\frac{f_r(D_o - 2t_o)h + 2nA_R\sigma_R}{2t_o h} \tag{4b}$$

where $\sigma_{\theta,o}$ is the hoop tensile stress acting in the outer tube in the circumferential direction; σ_R is the tensile stress acting in the external rings; n is the number of steel rings provided as external confinement; A_R is the cross-section area of each steel ring; h is the overall height of column. For unconfined CFDST column, $A_R = 0$. Both $\sigma_{\theta,o}$ and σ_R increase as the applied axial load increases. The value of $\sigma_{\theta,o}$ and σ_R will follow the stress-strain curve of the steel tube and rings respectively. Since the outer and inner tubes were subjected to a bi-axial stress state, the axial stress of the outer f_o and inner f_i tubes will not be the same as the uni-axial yield strength f_y. To determine the value of f_o and f_i, it can be reasonably assumed that the inner and outer steel tubes would yield at the maximum load-carrying capacity such that f_o and f_i can be determined by the von Mises yield criterion expressed in Eq. (5)

$$f_o^2 - f_o\sigma_{\theta,o} + \sigma_{\theta,o}^2 = f_{y,o}^2 \tag{5a}$$

$$f_i^2 - f_i\sigma_{\theta,i} + \sigma_{\theta,i}^2 = f_{y,i}^2 \tag{5b}$$

where $f_{y,o}$ and $f_{y,i}$ are the uni-axial yield strength of the outer and inner tubes respectively. For the core concrete, the confined concrete stress f_{cc} can be calculated by the commonly adopted formula as shown in Eq. (6)

$$f_{cc} = f_c' + kf_r \tag{6}$$

where f_c' is unconfined concrete cylinder strength and k is a constant taken as 4.1 (Cusson and Paultre 1994).

Substituting Eqs. (2), (4), (5) and (6) into Eq. (1), the total axial load- capacity of the CFDST column can be expressed as a function of the confining pressure f_r , materials' properties and other geometric parameters as shown in Eq. (7).

$$N = A_i\frac{\frac{f_r D_i}{2t_i} + \sqrt{\left(\frac{f_r D_i}{2t_i}\right)^2 - 4\left[\left(\frac{f_r D_i}{2t_i}\right)^2 - f_{y,j}^2\right]}}{2} \tag{7}$$

$$+A_o\frac{\left(-\frac{f_r(D_o - 2t_o)h + 2nA_R\sigma_R}{2t_o h}\right) + \sqrt{\left(-\frac{f_r(D_o - 2t_o)h + 2nA_R\sigma_R}{2t_o h}\right)^2 - 4\left[\left(-\frac{f_r(D_o - 2t_o)h + 2nA_R\sigma_R}{2t_o h}\right)^2 - f_{y,o}^2\right]}}{2}$$

$$+A_{cc}(f_c' + 4.1f_r)$$

The maximum axial load-carrying capacity of the CFDST columns can be obtained by evaluating the confining pressure $f_{r,o}$ that occurs at the maximum axial load-carrying capacity by solving in Eq. (8)

$$\frac{\partial N}{\partial f_r} = 0 \tag{8}$$

Table 4 Comparison between theoretical and experimental results (* and ** indicate ring-confined and unconfined specimens respectively)

Specimen label	Predicted axial strength N_{EC} (kN)	Predicted axial strength N_p (kN)	Experimentally measured axial strength N_t (kN)	$\frac{N_{EC}}{N_t}$	$\frac{N_p}{N_t}$	References
D-50-5-5*	2474	3081	3464	0.714	0.889	
D-50-5-10*	2474	2892	3107	0.796	0.931	
D-50-5-15*	2474	2820	2971	0.833	0.949	
D-50-5-20*	2474	2785	---#	---#	---#	
Average				0.781	0.923	
standard deviation				0.061	0.025	
D-50-5-0**	2474	2647	2852	0.867	0.928	
A1-1**	269	277	283	0.951	0.979	(Wei, Mau, Vipulanandan, & Mantrala, 1995)
A1-2**	258	265	285	0.905	0.930	
A2-1**	316	330	348	0.908	0.948	
A2-2**	303	312	348	0.871	0.897	
A3-1**	353	365	395	0.894	0.924	
A3-2**	355	367	395	0.899	0.929	
B1-1**	323	332	330	0.979	1.006	
B1-2**	314	323	335	0.937	0.964	
B2-1**	363	374	386	0.940	0.969	
B2-2**	366	377	395	0.927	0.954	
C1-1**	359	368	378	0.950	0.974	
C1-2**	354	363	385	0.919	0.943	
C2-1**	395	406	432	0.914	0.940	
C2-2**	388	398	408	0.951	0.975	
D1-1**	292	295	283	1.032	1.042	
D2-1**	256	261	299	0.856	0.873	
D3-1**	321	325	357	0.899	0.910	
D4-1**	364	369	380	0.958	0.971	
D5-1**	416	426	443	0.939	0.962	
D6-1**	631	658	644	0.980	1.022	
E1-1**	350	355	357	0.980	0.994	
E2-1**	455	461	477	0.954	0.966	
E3-1**	385	387	417	0.923	0.928	
E4-1**	619	631	598	1.035	1.055	
E5-1**	541	544	551	0.982	0.987	
E6-1**	487	490	524	0.929	0.935	
cc2a**	1631	1818	1790	0.911	1.016	(Tao, Han, & Zhao, 2004)
cc3a**	1548	1669	1648	0.939	1.013	
cc5a**	808	883	904	0.894	0.977	
cc6a**	2339	2525	2421	0.966	1.043	
cc7a**	3189	3414	3331	0.957	1.025	
Average				0.936	0.968	
standard deviation				0.042	0.044	

#Result is NOT included because of poor concrete compaction.

The obtained value of $f_{r,o}$ is then substituted into Eq. (7) to obtain the maximum axial load-carrying capacity of the CFDST column. Verification of the proposed analytical model with measured axial strength of CFDST columns by experimental test will be described next.

4.2 Verification with experimental results

The theoretical axial load-carrying capacities of the tested CFDST columns specimens evaluated by the proposed analytical model are listed in Table 4. The analytical model has also been applied to evaluate the theoretical axial load-carrying capacity of CFDST columns tested by other previous researchers (Wei *et al*. 1995a, 1995b, Tao *et al*. 2004). Both results were compared with the predicted uni-axial strength as per Eurocode 4 Part 1-1 (EC4 2004) in the same table. However, it should be noted that since the formula in Eurocode 4 does not take into account the effect of external confinement, the predicted uni-axial load-carrying capacities for unconfined and confined CFDST columns are the same.

In the table, N_p is the theoretical axial load-carrying capacity evaluated by the proposed model; N_{EC} is the theoretical axial load-carrying capacity evaluated by the design guidelines specified in Eurocode 4 Part 1-1 (EC4 2004); N_t is the experimentally measured axial load-carrying capacity in this study or by other previous researchers (Wei *et al*. 1995a, 1995b, Tao *et al*. 2004). From the table, it is observed that:

(1) The average value and standard deviation of the N_p/N_t ratio for ring-confined CFDST columns are 0.923 and 0.025 respectively. The maximum differences in the load-carrying capacity predicted by the proposed model and the test results (from authors and other researchers') are about −11.1% (underestimation) and −5.1% (underestimation).

(2) The average value and standard deviation of the N_p/N_t ratio for unconfined CFDST columns are 0.968 and 0.044 respectively obtained from the comparison. The maximum differences in the load-carrying capacity predicted by the proposed model and the test results (from authors and other researchers') are about −12.7% (underestimation) and +5.5% (overestimation).

(3) The average value and standard deviation of the N_{EC}/N_t ratio for unconfined CFDST columns are 0.936 and 0.043 respectively obtained from the comparison. The maximum differences in the load-carrying capacity predicted by the design guidelines specified in Eurocode 4 Part 1-1 (EC4 2004) and the test results (from authors and other researchers') are about −14.4% (underestimation) and +3.5% (overestimation). However, the difference in the predicted and measured strength increases as the content of ring confinement increases. The average value and standard deviation of the N_{EC}/N_t ratio for confined CFDST columns are 0.781 and 0.061 respectively. The maximum difference is about −28.6% (underestimation).

From the above, it is seen that the proposed model can predict fairly accurately the uni-axial load-carrying capacity of both unconfined and confined CFDST columns. In particular, the proposed model can predict more accurately the axial load-carrying capacity of ring-confined CFDST columns than the Eurocode.

5. Conclusions

Four CFDST columns with external confinement were tested under uni-axial compressive load. The performance of these CFDST columns were compared to those of four CFST columns, which have the same equivalent cross-section area, in terms of axial load-carrying capacity, elastic strength and elastic stiffness. To improve the confinement effectiveness of the steel tubes, both types of columns were confined with various spacing of external steel rings (spacing of $5t$, $10t$, $15t$ and $20t$, where t is the thickness of the steel tube). On the other hand, one CFDST column and one CFST column without installing external rings were also tested for comparison purpose.

From the test results, it was observed that:

(1) The load-carrying capacity (taken as the measured load at 0.05 axial strain) increases as the spacing of rings reduces due to the larger confining pressure provided to the in-filled concrete.

(2) The confining pressure developed more rapidly in CFDST columns than that in CFST column with the same equivalent cross-section area.

(3) Both elastic strength (taken as the measured load at 0.2% strain) and the load-carrying capacity of CFDST columns are larger than the CFST column counterparts. The improvement is about 33.4% and 7.8% on average respectively.

(4) The measured elastic stiffness of CFDST columns is larger than the CFST column counterparts. The improvement is about 25.8% on average.

(5) The strength of CFDST columns degrade more rapidly at high axial strain mainly because of the abrupt load transfer from the inner column during failure. No rapid strength degradation was observed in CFST columns.

Lastly, a theoretical model for predicting the axial load-carrying capacity of confined CFST columns has been proposed. The model was developed by considering the confining pressure provided by both the steel tubes and the ring confinement (if any) to the in-filled concrete. An equation expressing the axial-loading carrying capacity of unconfined or confined CFDST columns in terms of confining pressure and geometric parameters was derived. The validity of the model has been verified by comparing the theoretically predicted load-carrying capacity with the test results obtained by the authors and other researchers and those predicted by the Eurocode. From the comparison, it was evident that the proposed model can predict the measured axial-load carrying capacity of unconfined and confined CFDST columns fairly accurately. In particular, the proposed model can predict significantly more accurately the axial load-carrying capacity of confined CFDST columns than the Eurocode.

Acknowledgement

The work described in this paper has been substantially supported by a grant from the Research Grants Council of the Hong Kong Special Administrative Region, China (Project No. HKU 712310E). Technical supports for the experimental tests provided by the laboratory staff of the Department of Civil Engineering, The University of Hong Kong, are gratefully acknowledged.

References

Bechtoula, H., Kono, S. and Watanabe, F. (2009), “Seismic performance of high strength reinforced concrete columns”, *Structural Engineering and Mechanics*, **31**(6), 697-716.

Bindhu, K.R., Jaya, K.P. and Manicka Selvam, V.K. (2008), “Seismic resistance of exterior beam-column joints with non-conventional confinement reinforcement detailing”, *Structural Engineering and Mechanics*, **30**(6), 733-761.

Cai, J. and He, Z.Q. (2006), “Axial load behavior of square CFT stub column with binding bars”, *Journal of Constructional Steel Research,* **62**(5), 472-483.

Choi, S.M., Jung, D.S., Kim, D.J. and Kim, J.H. (2007), “An evaluation equation of load capacities for CFT

square column-to-beam connections with combined diaphragm", *Steel and Composite Structures*, **7**(4), 303-320.
Cusson, D. and Paultre, P. (1994), "High-strength concrete columns confined by rectangular ties", *Journal of Structural Engineering*, *ASCE*, **120**(3), 783-804.
Dai, X. and Lam, D. (2010), "Axial compressive behaviour of stub concrete-filled columns with elliptical stainless steel hollow sections", *Steel and Composite Structures*, **10**(6), 517-539.
EC4, Eurocode 4 (2004), Eurocode 4: *Design of composite steel and concrete structures: Part 1-1: General rules and rules for buildings*, UK.
Elchalakani, M., Zhao, X.L. and Grzebieta, R. (2002), "Tests on concrete filled double-skin (CHS outer and SHS inner) composite short columns under axial compression", *Thin-walled Structures*, **40**(5), 415-441.
Fang, Y.F. and Zhu, L.T. (2009), "Recycled aggregate concrete filled steel SHS beam-columns subjected to cyclic loading", *Steel and Composite Structures*, **9**(1), 19-38.
Ferretti, E. (2004), "On Poisson ratio and volumetric strain in concrete", *International Journal of Fracture*, **126**, 49-55.
Han, L.H., Tao, Z., Huang, H. and Zhao, X.L. (2004), "Concrete-filled double skin (SHS outer and CHS inner) steel tubular beam-columns", *Thin-walled structures,* **42**(9), 1329-1355.
Han, L.H., Huang, H. and Zhao, X.L. (2009), "Analytical behaviour of concrete-filled double skin steel tubular (CFDST) beam-columns under cyclic loading", *Thin-walled structures,* **47**(6-7), 668-680.
Ho, J.C.M., Lam, J.Y.K. and Kwan, A.K.H. (2010), "Effectiveness of adding confinement for ductility improvement of high-strength concrete columns", *Engineering Structures*, **32**(3), 714-725,
Ho, J.C.M., Lam, J.Y.K. and Kwan, A.K.H. (2012), "Flexural ductility and deformability of concrete beams incorporating high-performance materials", *The Structural Design of Tall and Special Buildings*, **21**(2), 114-132.
Ho, J.C.M. (2011), "Inelastic design of high-axially loaded concrete columns in moderate seismicity regions", *Structural Engineering and Mechanics*, **39**(4), 559-578.
Hsu, H.L., Juang, J.L. and Luo, K.T. (2009), "Experimental evaluation on the seismic performance of high strength thin-walled composite members accounting for sectional aspect ratio effect", *Steel and Composite Structures*, **9**(4), 367-380.
Hu, H.T., Su, F.C. and Elchalakani, M. (2010), "Finite element analysis of CFT columns subjected to pure bending moment", *Steel and Composite Structures*, **10**(5), 415-428.
Huang, Y., Long, Y. and Cai, J. (2008), "Ultimate strength of rectangular concrete-filled steel tubular (CFT) stub columns under axial compression", *Steel and Composite Structures*, **8**(2), 115-128.
Lam, J.Y.K., Ho, J.C.M. and Kwan, A.K.H. (2009a), "Flexural ductility of high-strength concrete columns with minimal confinement", *Materials and Structures*, **42**(7), 909-921.
Lam, J.Y.K., Ho, J.C.M. and Kwan, A.K.H. (2009b), "Maximum axial load level and minimum confinement for limited ductility design of concrete columns", *Computers and Concrete*, **6**(5), 357-376.
Lee, S.J. (2007), "Capacity and the moment-curvature relationship of high-strength concrete filled steel tube columns under eccentric loads", *Steel and Composite Structures*, **7**(2), 135-160.
Liew, J.Y.R. and Sohel, K.M.A. (2009), "Lightweight steel-concrete-steel sandwich system with J-hook connectors", *Engineering Structures*, **31**(5), 1166-1178.
Liew, J.Y.R., Sohel, K.M.A. and Koh, C.G. (2009), "Impact tests on steel-concrete-steel sandwich beams with lightweight concrete core", *Engineering Structures*, **31**(9), 2045-2059.
Liew, J.Y.R. and Sohel, K.M.A. (2010), "Structural Performance of steel-concrete-steel sandwich composite structures", *Advances in Structural Engineering*, **13**(3), 453-470.
Lu, X. and Hsu, C.T.T. (2007), "Tangent Poisson's ratio of high-strength concrete in triaxial compression", *Magazine of Concrete Research*, **59**(1), 69-77.
Lu, X. and Zhou, Y. (2007), "An applied model for steel reinforced concrete columns", *Structural Engineering and Mechanics*, **27**(6), 697-711.
Mander, J.B., Priestley, M.J.N. and Park, R. (1988), "Theoretical stress-strain model for confined concrete", *Journal of Structural Engineering, ASCE*, **114**(8), 1804-1825.
Pam, H.J. and Ho, J.C.M. (2001), "Flexural strength enhancement of confined reinforced concrete columns", *Proceedings*, *Institution of Civil Engineers*, *Structures and Buildings*, **146**(4), 363-370.
Pam, H.J. and Ho, J.C.M. (2009), "Length of critical region for confinement steel in limited ductility high-

strength reinforced concrete columns", *Engineering Structures*, **31**(12), 2896-2908.
Park, J.W., Hong, Y.K. and Choi, S.M. (2010), "Behaviors of concrete filled square steel tubes confined b carbon fiber sheets (CFS) under compression and cyclic loads", *Steel and Composite Structures*, **10**(2), 187-205.
Persson, B. (1999), "Poisson's ratio of high-performance concrete", *Cement and Concrete Research*, **29**(10), 1647-1653.
Sohel, K.M.A. and Liew, J.Y.R. (2011), "Steel-concrete-steel sandwich slabs with lightweight core – static performance", *Engineering Structures*, **33**(3), 981-992.
Sadjadi, R. and Kianoush, M.R. (2010), "Application of fiber element in the assessment of the cyclic loading behavior of RC columns", *Structural Engineering and Mechanics*, **34**(3), 301-317.
Tao, Z., Han, L.H. and Zhao, X.L. (2004), "Behaviour of concrete-filled double skin (CHS inner and CHS outer) steel tubular stub columns and beam-columns", *Journal of Constructional Steel Research,* **60**(8), 1129-1158.
Tao, Z., Han, L.H. and Wang, D.Y. (2007), "Experimental behaviour of concrete-filled stiffened thin-walled steel tubular columns', *Thin-walled structures,* **45**(5), 517-527.
Uenaka, K., Kitoh, H. and Sonoda, K. (2010), "Concrete filled double skin circular stub columns under compression", *Thin-Walled Structures*, **48**(1), 19-24.
Wei, S., Mau, S.T., Vipulanandan, C. and Mantrala, S.K. (1995a), "Performance of new sandwich tube under axial loading: experiment", *Journal of Structural Engineering*, **121**(12), 1806-1814.
Wei, S., Mau, S.T., Vipulanandan, C. and Mantrala, S.K. (1995b), "Performance of new sandwich tube under axial loading: analysis", *Journal of Structural Engineering*, **121**(12), 1815-1821.
Yan, Z.H. and Au, F.T.K. (2010) "Nonlinear dynamic analysis of frames with plastic hinges at arbitrary locations", *The Structural Design of Tall and Special Buildings*, **19**(7), 778-801.
Yang, Y. and Han, L.H. (2008), "Concrete-filled double-skin tubular columns under fire", *Magazine of Concrete Research,* **60**(3), 211-222.
Young, B. and Ellobody, E. (2006), "Experimental investigation of concrete-filled cold formed high-strength stainless steel tube columns", *Journal of Constructional Steel Research,* **62**(5), 484-492.
Zhang, G., Liu, B., Bai, G. and Liu, J. (2009), "Experimental study on seismic behavior of high strength reinforced concrete frame columns with high axial compression ratios", *Structural Engineering and Mechanics*, **33**(5), 653-656.
Zhao, X.L. and Grzebieta, R. (2002), "Strength and ductility of concrete filled double skin (SHS inner and SHS outer) tubes", *Thin-walled structures,* **40**(2), 199-213.
Zhao, X.L., Tong, L.W., and Wang, X.Y. (2010). CFDST stub columns subjected to large deformation axial loading. *Engineering Structures,* **32**(3), 692-703.
Zhou, X.M., Wu, Y.F. and Leung, A.Y.T. (2012), "Analyses of plastic hinge regions in reinforced concrete beams under monotonic loading", *Engineering Structures*, **34**, 466-482.
Zhou, K.J.H., Ho, J.C.M. and Su, R.K.L. (2010), "Normalised rotation capacity for deformability evaluation of high-performance concrete beams", *Earthquakes and Structures*, **1**(3), 269-287.

CC

List of notations

CFST : Concrete-filled-steel-tubular
CFDST : Double-skinned Concrete-filled-steel-tubular
D_i : Outer diameter of inner tube of CFDST column
D_o : Outer diameter of outer tube of CFST/CFDST column
t_i : Thickness of inner tube of CFDST column
t_o : Thickness of outer tube of CFDST column
A_i : Cross-section area of the inner tube

A_o	: Cross-section area of the outer tube
A_{cc}	: Cross-section area of the core concrete
A_R	: Cross-section area of external steel ring
N	: Load-carrying capacity of a specimen
N_i	: Axial load taken by the inner tube
N_o	: Axial load taken by the outer tube
N_{cc}	: Axial load taken by the core concrete
N_{EC}	: Axial strength of a specimen evaluated by Eurocode
N_p	: Axial strength of a specimen predicted by the proposed model
N_t	: Experimentally measured axial strength of a specimen
f_i	: Axial stress of the inner tube
f_o	: Axial stress of the outer tube
f_{cc}	: Axial stress of the core concrete
f_c'	: Uni-axial concrete compressive strength represented by cylinder strength
f_r	: Confining pressure
$\sigma_{\theta, i}$	: Hoop stress in inner tube of CFDST column
$\sigma_{\theta, o}$	: Hoop stress in outer tube of CFDST column
σ_R	: Tensile stress in external steel ring
$f_{y, ,}$	: Yield strength of inner tube of CFDST column
$f_{y, ,}$	: Yield strength of outer tube of CFDST column
f_R	: Yield strength of external steel ring
n	: Number of external steel bars
h	: Height of the specimen
LVDT	: Linear variable displacement transducer